Assessing sequence plasticity of a virus-like nanoparticle by evolution toward a versatile scaffold for vaccines and drug delivery

Yuan Lu[a], Wei Chan[a], Benjamin Y. Ko[a], Christopher C. VanLang[a], and James R. Swartz[a,b,1]

[a]Department of Chemical Engineering, Stanford University, Stanford, CA 94305; and [b]Department of Bioengineering, Stanford University, Stanford, CA 94305

Edited by David A. Tirrell, California Institute of Technology, Pasadena, CA, and approved August 26, 2015 (received for review May 29, 2015)

Virus-like particles (VLPs) have been extensively explored as nanoparticle vehicles for many applications in biotechnology (e.g., vaccines, drug delivery, imaging agents, biocatalysts). However, amino acid sequence plasticity relative to subunit expression and nanoparticle assembly has not been explored. Whereas the hepatitis B core protein (HBc) VLP appears to be the most promising model for fundamental and applied studies; particle instability, antigen fusion limitations, and intrinsic immunogenicity have limited its development. Here, we apply *Escherichia coli*-based cell-free protein synthesis (CFPS) to rapidly produce and screen HBc protein variants that still self-assemble into VLPs. To improve nanoparticle stability, artificial covalent disulfide bridges were introduced throughout the VLP. Negative charges on the HBc VLP surface were then reduced to improve surface conjugation. However, removal of surface negative charges caused low subunit solubility and poor VLP assembly. Solubility and assembly as well as surface conjugation were greatly improved by transplanting a rare spike region onto the common shell structure. The newly stabilized and extensively modified HBc VLP had almost no immunogenicity in mice, demonstrating great promise for medical applications. This study introduces a general paradigm for functional improvement of complex protein assemblies such as VLPs. This is the first study, to our knowledge, to systematically explore the sequence plasticity of viral capsids as an approach to defining structure function relationships for viral capsid proteins. Our observations on the unexpected importance of the HBc spike tip charged state may also suggest new mechanistic routes toward viral therapeutics that block capsid assembly.

virus-like particle | engineered nanoparticles | disulfide stabilization | hepatitis core protein | cell-free protein synthesis

Virus-like particles (VLPs) are probably the most precisely defined and, therefore, potentially the most useful complex nanometer-scale scaffolds (1). VLPs mimic the capsid structure of real viruses, but lack infectious genetic material. Selected VLPs derived from pathogens have already provided major advances in the development of vaccines that have known and relatively homogeneous structures as well as enhanced immunogenicity (2). Such nanoparticles provide comparable cellular uptake and intracellular trafficking compared with natural viruses (3), and also have repetitive surfaces for the high-density display of vaccine antigens (4). In addition, VLPs offer favorable trafficking from the injection site to lymph nodes (5). Since the first reported use of a hepatitis B core protein (HBc) VLP as an antigen carrier in 1987 (6), at least 110 VLP vaccine candidates have been constructed by using capsid proteins from 35 different viral families (7).

Among different types of VLPs, the HBc VLP is the most flexible and promising model for fundamental and applied immunological studies (8). One advantage of the HBc VLP platform is that the capsids can be produced by using the simple *Escherichia coli* host system (7). In previous studies, researchers mainly focused on engineering HBc protein for the display of different vaccine antigens by using a fusion protein approach. However, after nearly 30 y of HBc VLP-antigen vaccine development, there is still no approved vaccine, and only a few have entered phase III clinical trials. We suggest that three main factors limit their development: core protein capsid assembly instability, reduced VLP assembly of core protein/antigen fusion proteins, and intrinsic immunogenicity. In addressing these limitations, we also sought to carefully define the HBc VLP amino acid sequence plasticity relative to VLP producibility and functional versatility.

To better define these challenges, it is helpful to consider how the HBc capsid is natively synthesized. In the replication cycle of the hepatitis B virus (HBV) (Fig. 1*A*), the HBV virion is internalized into the hepatocyte, and the inner core breaks out of the envelope (9). The HBV core particle migrates to the nucleus and disassembles to release the viral genome, which is then repaired and transcribed. The viral mRNA is next translated in the cytoplasm to produce the viral core and other proteins. The HBV core particle must then assemble and bud into the endoplasmic reticulum to be enveloped and exported from the cell. Thus, the HBc capsid has not evolved to be an independent particle but has evolved to simultaneously load its nucleic acid cargo during assembly, to be stabilized by the outer viral coat, and to then open and release its cargo after infection. It seems reasonable then to assume that viral assembly stability is conferred both by the nucleic acid cargo and by the lipid and surface protein coating. We therefore suggest that our data showing poor assembly stability for empty core protein VLPs is not

Significance

Particle instability, antigen fusion limitations, and intrinsic immunogenicity greatly limit the development of virus-like particles (VLPs). To address these problems, the Hepatitis B core protein (HBc) VLP was extensively modified to improve its functional properties by introducing an artificial disulfide network, removing the surface charge, and transplanting a new surface spike region. This study systematically explores the plasticity of viral capsids and, thereby, expands our knowledge regarding the relevant structure function relationships. Notably, we uncovered the influence of the HBc spike and its negative charges on capsid assembly and immunogenicity. Our observations on the unexpected importance of the HBc spike tip charged state suggest unexplored mechanisms for antiviral therapeutics that block capsid assembly.

Author contributions: Y.L. and J.R.S. designed research; Y.L., W.C., B.Y.K., and C.C.V. performed research; Y.L., W.C., B.Y.K., and C.C.V. contributed new reagents/analytic tools; Y.L. and J.R.S. analyzed data; and Y.L. and J.R.S. wrote the paper.

The authors declare no conflict of interest.

This article is a PNAS Direct Submission.

[1]To whom correspondence should be addressed. Email: jswartz@stanford.edu.

This article contains supporting information online at www.pnas.org/lookup/suppl/doi:10.1073/pnas.1510533112/-/DCSupplemental.

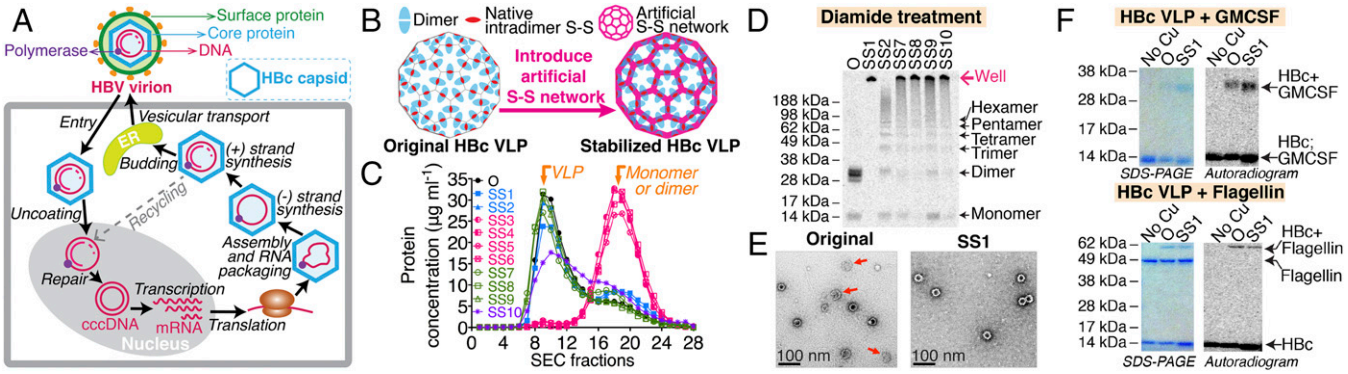

Fig. 1. Synthesis and functional verification of stabilized HBc VLPs with correct disulfide bonds. (*A*) Schematic of the replication cycle of HBV. (*B*) Schematic for the introduction of an artificial disulfide (S-S) bond network. (*C*) SEC analysis of stabilized VLPs. O, original HBc. (*D*) The nonreducing SDS/PAGE and the autoradiogram analysis after the oxidization treatment of purified VLPs. (*E*) TEM images of VLPs. Arrows indicate VLPs that are not fully assembled. (*F*) Reducing SDS/PAGE analysis of click-reaction products. Cu(I) was not added to the reaction as the control. HBc VLPs (monomer: 16.7 kDa) were radioactive. Flagellin (52.7 kDa) and GMCSF (16.1 kDa) were not radioactive.

surprising and may help explain why many HBc/antigen fusion proteins suffer from poor assembly.

Another concern is that preexisting HBc-specific antibodies might interfere with HBc-antigen vaccination or that the intrinsically strong immunogenicity of the HBc core protein might suppress the immunogenicity of conjugated antigens. To promote development of HBc VLP-antigen vaccines, we sought to develop new approaches to overcome these problems.

We propose that a versatile VLP vaccine and delivery scaffold should: (*i*) self-assemble independent of cargo or other assistance; (*ii*) present ordered and consistently oriented antigens much like natural viruses; (*iii*) offer selectively engineered immune stimulation; (*iv*) be well dispersed and stable in solution during modification, formulation, storage, administration, and trafficking to lymph nodes, and (*v*) have low immunogenicity. To provide these functional attributes, we explored the amino acid sequence plasticity of this VLP to illuminate structure function relationships that govern the consistent assembly of 240 polypeptide subunits into a hollow 35-nm diameter nanoparticle as a robust and versatile scaffold for vaccine and delivery applications.

Results and Discussion

Stabilizing the VLPs. The HBc polypeptide truncated at amino acid 149 has been shown to predominantly form (>95%) $T = 4$ VLPs (10). Two HBc monomers (16.7 kDa) associate into a compact dimer (33.5 kDa) with a potential intermolecular disulfide bond between the Cys-61 residues of the two monomers. Dimers (120 copies) self-assemble into the $T = 4$ VLP by weak interactions (*SI Appendix*, Fig. S1*A*). After assembly, the surface of the HBc VLP displays an ordered array of 120 spikes (projecting alpha helices), which can be exploited for the display of foreign molecules (8). The $T = 4$ icosahedral capsid has 12 regular pentameric faces and 30 regular hexameric faces (*SI Appendix*, Fig. S1*B*). Each pentamer is surrounded by five hexamers (*SI Appendix*, Fig. S1*C*).

Recently, an *Escherichia coli*-based cell-free protein synthesis (CFPS) system was successfully developed for the production and modification of VLPs (11, 12). CFPS enables rapid production of VLPs at high yields (~0.5 g/L) in a few hours. This technology has been shown to be scalable from the microliter to the 100-L scale (13). Taking advantage of the open CFPS environment, nonnatural amino acids (nnAAs) can be readily introduced into VLPs (11), allowing for the conjugation of functional molecules to the VLP outer surface. These advantages eliminate the need for disassembly and reassembly or chemical modification after VLP production.

Because of the multiple concerns arising from nanoparticle instability, we sought to strengthen the VLP structure. Disulfide (S-S) bonds already stabilize the dimers. Introducing new S-S bridges to cross-link the pentamers and hexamers would therefore totally stabilize the VLP (Fig. 1*B*). To form stable VLPs, we searched for cysteine introduction locations that would offer consistent S-S bond formation at both pentameric and hexameric junctions. We devised two strategies. The first was to look for two amino acids with the shortest distances between side chains of interacting dimers (*SI Appendix*, Fig. S1 *D* and *E*). The second was to look for opportunities to form S-S bonds between the relatively disordered C termini of the monomers. In total, 10 pairs of mutations were evaluated, including SS1 (D29C-R127C) and SS2 (T109C-V120C) at the assembly interfaces and SS3 (Y132C-N136C), SS4 (Y132C-A137C), SS5 (R133C-N136C), SS6 (R133C-A137C), SS7 (P134C-P135C), SS8 (P134C-N136C), SS9 (P134C-A137C), and SS10 (P135C-N136C) to connect the C termini.

To ensure the formation of proper S-S bonding in VLPs, HBc proteins were first synthesized in a reducing environment using the CFPS system (*SI Appendix*, Fig. S2*A*). The HBc monomer can self-assemble into a VLP in the CFPS reaction solution by using a subsequent dialysis process (*SI Appendix*, Fig. S2 *B* and *C*) to increase the ionic strength and enhance the hydrophobic interactions between the assembly interfaces presented by the dimers. The HBc dimers self-assembled into VLPs most effectively when the molar concentration of NaCl was increased to 0.5 M or above (*SI Appendix*, Fig. S2*D*). Assembly and purification by size-exclusion chromatography (SEC) were conducted in a reducing environment to avoid the formation of incorrect S-S bonds. The mutants SS3, SS4, SS5, and SS6 did not assemble into VLPs (Fig. 1*C*). The purified fractions (SEC fractions 9–11) of assembled VLPs were then oxidized to form S-S bonds by adding 20 mM diamide (*SI Appendix*, Fig. S2*E*). We reasoned that fully cross-linked VLPs would be stable even in SDS and would fail to enter an SDS/PAGE gel (Fig. 1*D*). Only oxidized SS1 particles completely remained in the loading well of the SDS/PAGE gel although SS7–SS10 were also significantly stabilized. The cysteines introduced for SS1 occur in the middle of the principle dimer-to-dimer interface (as opposed to the more C-terminal locations). The consistent proximity of these paired cysteines probably explains the more complete stabilization. Based on these results, mutant SS1 was chosen for further development. Sucrose gradient centrifugation confirmed proper assembly (*SI Appendix*, Fig. S2*F*). An additional benefit is that the S-S bonds can confer conditional stability such that the nanoparticle can still open under the reducing environment inside the cell for delivery applications (*SI Appendix*, Fig. S2*G*).

To further evaluate the HBc SS1 VLP, its stability was compared with that of the original HBc VLP. Transmission electron microscope (TEM) images (Fig. 1*E*) demonstrated that the original HBc VLP either did not fully assemble or disassembled during

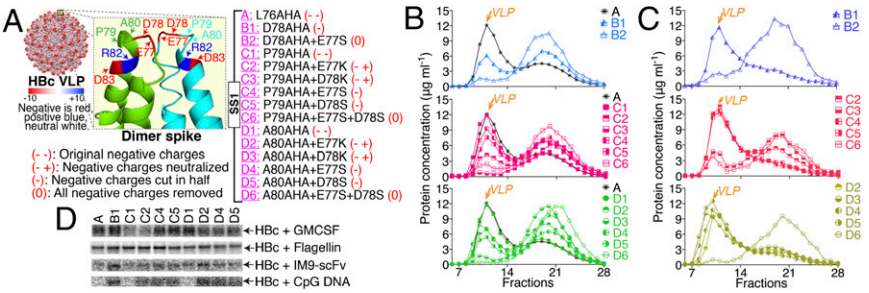

Fig. 2. HBc VLP mutants with reduced negative surface charges. (*A*) The charge distribution of the HBc VLP surface at physiological pH, the distribution of charged amino acids in the dimer spike, and mutations for reducing or removing the negative charges of the HBc VLP surface. All of these mutations were based on mutant SS1. (*B*) The SEC profiles after dialysis against buffer with 0.5 M NaCl. (*C*) SEC results after dialysis against 1.5 M NaCl. (*D*) The reducing SDS/PAGE autoradiograms of the click-reaction products. The column labels refer to the VLPs listed in *A*.

sample preparation, whereas HBc SS1 VLPs appeared as uniform, fully assembled capsids. We also evaluated stability during incubation under physiological condition. Approximately 50% of the original HBc VLPs disassembled when incubated in physiological PBS buffer overnight, and almost all disassembled when incubated in a low ionic strength buffer (*SI Appendix*, Fig. S2*H*). However, the HBc SS1 VLP was stable in all of the conditions tested. The HBc SS1 VLP also showed much better stability after a freeze-thaw cycle than the original HBc VLP (*SI Appendix*, Fig. S2*I*). Overall, the artificial S-S network in the HBc SS1 VLP confers excellent assembly stability.

Click chemistry conjugation reactions were then tested to further verify the functionality of the oxidized VLPs. Flagellin and GMCSF were used as example proteins for conjugation. CFPS provides a facile means for site-specific introduction of nnAAs with an alkyne moiety into flagellin (HPG, homopropargylglycine) (11) and GMCSF (PPF, *p*-propargyloxy-phenylalanine) (14), as well as a nnAA with an azide moiety (AHA, azidohomoalanine) into the L76 site near the tip of the spike region on the VLP surface. This approach enabled the direct coupling of flagellin and GMCSF to the VLPs by using Cu(I)-catalyzed [3+2] cycloaddition click chemistry (*SI Appendix*, Fig. S2 *J* and *K*). The reaction results (Fig. 1*F*) showed that flagellin and GMCSF were readily conjugated to the HBc SS1 VLP.

Engineering the VLP Surface. At physiological pH, the surface of the HBc VLP is negatively charged as shown in Fig. 2*A*. The HBc VLP surface is dominated by 120 protruding dimer spikes that serve as obvious attachment sites with high steric availability. However, they are terminated with four negatively charged amino acids (E77 × 2, D78 × 2). Initial conjugation tests showed good attachment of GMCSF and flagellin to the stabilized VLPs but poor attachment of IM9-scFv (a lymphoma vaccine antigen) (15) and CpG DNA (an innate immunity stimulator) (16). The latter two molecules are characterized by negative charge density near the alkyne. We hypothesized that charge repulsion inhibited IM9-scFv and CpG attachment (*SI Appendix*, Fig. S3 *A* and *B*).

We therefore reasoned that decreasing the number of negative charges on the HBc VLP surface would allow good conjugation for most attachment molecules. There are three negatively charged amino acids (E77, D78, and D83) and one positively charged amino acid (R82) on the surface of the monomer spike. We assumed that D83 and R82 could, at least partially, neutralize each other so we targeted the negative charges at the tip of the dimer spike, E77 and D78. To reduce or remove net negative charge, we tested three strategies: reduce negative charge in half (E77S, D78S, or D78AHA), use positive charges to neutralize negative charges (E77K or D78K), or remove all negative charges (E77S+D78AHA or E77S+D78S). At the same time, different AHA sites on the dimer spike were tested. In total, 15 mutated forms of the HBc SS1 VLP were evaluated, as summarized in Fig. 2*A*.

Initial CFPS results showed that changing the AHA sites without decreasing the surface charge did not affect the HBc protein solubility. However, solubility of the accumulated product decreased greatly for the mutants in which negative surface charge was removed (*SI Appendix*, Fig. S3*C*). After dialysis against 0.5 M NaCl, the percent solubility of some mutants increased. SEC analyses showed that changing the AHA sites did not affect VLP assembly, but the charge change mutations reduced the VLP assembly efficiency dramatically (Fig. 2*B*). Because attractive hydrophobic interactions appear to guide specific interactions during VLP assembly (17), we hypothesized that higher ionic strength would enhance assembly. We saw that dialysis against 1.5 M NaCl greatly improved the VLP assembly efficiency for 11 of the 15 mutants (Fig. 2*C*). The exceptions are B2, C3, C6, and D6. Three of the four had both negative charges removed at the spike tip of each monomer. In an attempt to improve the percent solubility and the VLP assembly efficiency of B2, C3, C6, and D6, several approaches were examined (*SI Appendix*, Figs. S3–S8) including: modifying CFPS conditions (salts, metal ions, temperature, detergents); changing dialysis conditions (pH, temperature, detergents, salts in the Hofmeister series, amino acid additions); additional mutations (different disulfide bond network, F97L mutation); and the use of various protein refolding additives and conditions (denaturants, pH, redox environment, arginine, detergents). Notably, all attempts failed to improve the VLP assembly efficiency. These results suggest that negative charge at the spike tip of the dimer is important for VLP assembly. Although we could reduce surface negative charge in half (mutants B1, C4, and D4) and use positive charge to neutralize negative charge (mutants C2, D2, and D3), we could not remove all of the negative charge (mutations B2, C6, and D6).

Surface conjugation to these mutated VLPs was then tested. In addition to GMCSF and flagellin, we tested two molecules, IM9-scFv and CpG DNA, which display negative charge density near the alkyne functional group (*SI Appendix*, Fig. S3*B*). The conjugation reaction results (Fig. 2*D*) showed that decreasing surface negative charge greatly improved the conjugation efficiency for IM9-scFv and CpG DNA without reducing conjugation of GMCSF and flagellin. The mutant B1 provides the best overall conjugation efficiency and was preferred because it required only a single amino acid mutation. Mutant D2 may also be attractive because it provides good conjugation with better soluble production yields.

Transplanting a Rare HBc Spike. Reducing the HBc VLP surface charges improved the conjugation of displayed molecules, but production yields were relatively low for these mutated VLPs (*SI Appendix*, Fig. S3*C*). The best mutant for conjugation, B1, accumulated during expression with less than 50% solubility. Although optimization of CFPS and dialysis conditions improved solubility, those changes decreased VLP assembly efficiency (*SI Appendix*, Figs. S3–S6). These limitations led us to seek an

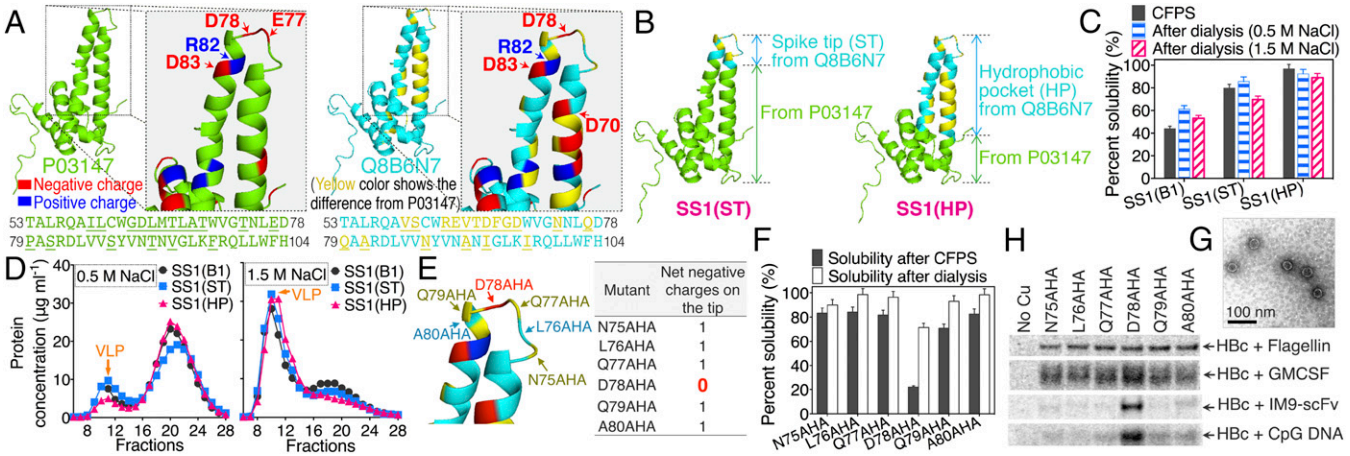

Fig. 3. New mutants produced by transplanting the spike region of the natural mutant, Q8B6N7, into HBc SS1. (*A*) The difference between the HBc protein used in this study (P03147) and a natural mutant (Q8B6N7). The amino acid sequences of the spike region are shown below the structure. The sequence differences are underlined and marked in yellow. (*B*) Illustration for the creation of two new mutants [SS1(ST) and SS1(HP)]. (*C*) The percent solubility of proteins after CFPS reactions and after dialysis. (*D*) SEC analysis after dialysis against buffer with 0.5 M NaCl or 1.5 M NaCl. (*E*) The six different conjugation sites tested on the SS1(HP) protein spike tip. (*F*) The percent solubility of proteins after CFPS reactions and after 1.5 M NaCl dialysis. (*G*) The TEM image of HBc SS1(HP) 78AHA VLP. (*H*) The reducing SDS/PAGE autoradiogram analysis of click-reaction products of HBc SS1(HP) VLP with flagellin, GMCSF, IM9-ScFv, and CpG DNA. Cu(I) was not added to the control reaction.

alternative approach for modifying the HBc dimer spike. Rational design and directed evolution are two general strategies for protein engineering. However, exploring all possible combinations of mutating only three amino acids would require testing of nearly 7,000 candidates, which was outside the scope of the current methods. Alternatively, we looked to find clues in naturally occurring viral mutants. In addition to improving VLP production and surface conjugation, we also sought to reduce concerns about the HBc VLP antigenicity and immunogenicity.

By examining HBc protein sequences from the UniProt database (18) and the hepatitis core family PF00906 sequences from the Pfam database (19), we found a few natural mutants with only one negatively charged amino acid (D78) on the monomer spike tip. However, none had both negative charges (E77, D78) removed, consistent with our mutational results (*SI Appendix*, Fig. S9). One natural mutant (UniProt accession no. Q8B6N7) was quite novel; Q8B6N7 has a natural mutation of E77Q, leaving one net negative charge at the 78 site. Comparing it to the rest of approximately 7,000 members of the hepatitis core family PF00906, Q8B6N7 was the only mutant heavily mutated throughout the spike domain. Fig. 3*A* compares the amino acid sequence of Q8B6N7 to that of a more conserved HBc protein (UniProt accession no. P03147).

To estimate the effects of the naturally selected mutations in Q8B6N7 on the functional characteristics of the VLP, the spike [either the spike tip (ST) or the whole hydrophobic pocket (HP)] from Q8B6N7 was transplanted into the SS1 mutant of P03147 to create two new mutants: SS1(ST) and SS1(HP) (Fig. 3*B*). The HP transplants allowed us to evaluate the effect of changing only the spike region while keeping the VLP shell the same. These two new mutants accumulated during expression with higher solubility than mutant SS1(B1) (Fig. 3*C*). However, SS1(ST) and SS1(HP) still did not self-assemble into VLPs after 0.5 M NaCl dialysis (Fig. 3*D*), supporting our initial observations of the importance of negative tip spike charges. As before, dialysis against buffer with a higher ionic strength (1.5 M NaCl) stimulated assembly of the mutated subunits into VLPs. These new VLPs were then separated by SEC and oxidized by diamide to form the disulfide-bond network. Proper assembly of the SS1(ST) and SS1(HP) VLPs was verified by nonreducing SDS/PAGE and sucrose gradient centrifugation (*SI Appendix*, Fig. S10). Because SS1(HP) had higher soluble accumulation yields than SS1(ST) (Fig. 3*C*), SS1(HP) was chosen for subsequent studies. We also reasoned that, with 18 mutations in the spike region, SS1(HP) would cause fewer antigenicity and immunogenicity concerns.

To identify the best conjugation site for SS1(HP), AHA was introduced individually at amino acid positions 75–80 (N75AHA, L76AHA, Q77AHA, D78AHA, Q79AHA, and A80AHA; Fig. 3*E*). These mutants were all stabilized by the new SS1 disulfide bridge (D29C-R127C). Introducing the nnAA at D78 is particularly attractive because it totally removes the negative charges at the tip. CFPS results indicated that all these mutants accumulated as mostly soluble product except mutant D78AHA (Fig. 3*F*). However, after dialysis against 1.5 M NaCl, the percent solubility of mutant D78AHA reached approximately 70%. SEC results showed that all these mutants self-assembled into VLPs (*SI Appendix*, Fig. S10). The VLPs were then separated by SEC and oxidized by diamide. TEM analysis showed that the size of the mutant SS1(HP) 78AHA VLP was correct (Fig. 3*G*). Importantly, the heavily mutated HP spike allowed assembly after removal of all of the spike tip charges in contrast to results with the more conserved spike.

Conjugation to these mutated VLPs was then tested with the four molecules previously evaluated: flagellin, GMCSF, IM9-ScFv, and CpG DNA, each with exposed alkynes. The conjugation reaction results (Fig. 3*H*) showed that the removal of surface negative charges on the HBc VLP greatly improved the conjugation efficiency of IM9-scFv and CpG DNA without reducing conjugation of GMCSF or flagellin. HBc SS1(HP) D78AHA was therefore chosen as the best VLP for further development. To address the possibility that the change to the hydrophobic pocket (HP) spike from Q8B6N7 might cause a different assembly stabilization disulfide bond to be superior in the shell, the different S-S positions (SS1–SS10) were again tested. SS1 was still the best (*SI Appendix*, Fig. S10 *H* and *I*), suggesting that the spike transplant did not significantly distort the shell structure.

Hydrophobic Interaction and Electrostatic Repulsion During HBc VLP Assembly. Attractive hydrophobic interactions have been thought to guide specific interactions during the assembly of viral capsids (17). However, in this study, the surface-exposed negative charges on the spike tip greatly influenced the assembly efficiency of the HBc subunits (Fig. 4*A*). Reducing the negative charges on the spike tip caused the formation of insoluble aggregates. It has been suggested that the electrostatic repulsion between the HBc spike tips provides a beneficial opposition to aid capsid assembly. Our observations (summarized in Fig. 4) suggest a critical

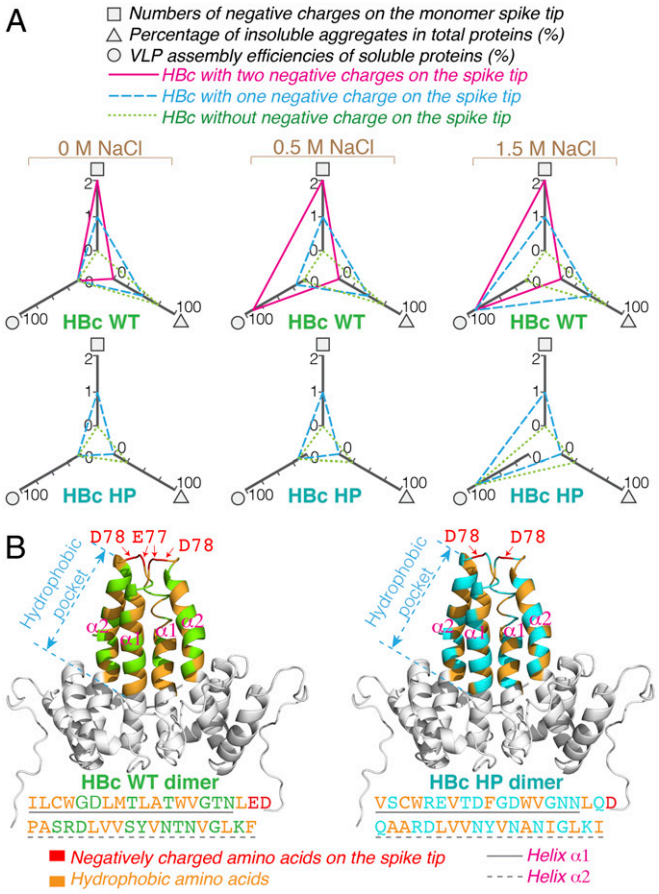

Fig. 4. Importance of electrostatic repulsion for HBc VLP assembly for wild-type (P03147) and HP spike (Q8B6N7) variants. (*A*) The radar charts summarize the effects of spike tip charges on HBc solubility and VLP assembly at different NaCl concentrations. (*B*) Intradimer hydrophobic interactions in HBc wild-type (WT) and HBc HP. The same amino acid sequences between HBc WT and HBc HP are marked as gray color in the structures. The amino acid sequences of the hydrophobic pockets are shown below the structure.

dynamic balance between hydrophobic attractions and electrostatic repulsions for correct HBc VLP assembly (at least in vitro). For simplicity, we do not consider the cases with nnAA introduction here. Reducing the negative charges on the spike tip may have allowed nonproductive hydrophobic interactions to cause aberrant aggregation. Increasing the ionic strength strengthens hydrophobic attractions, apparently allowing productive assembly interactions to dominate.

Fig. 4*B* compares the hydrophobic pocket of HBc WT protein with that of the HBc HP variant. Helices α1 and α2 (Fig. 4*B*) pack together to form a stable dimer by hydrophobic interactions (17). Although HBc WT and HBc HP have different hydrophobic residues in the dimeric hydrophobic pocket, the number of these attractive residues is similar: 20 for WT and 18 for the HP spike. We suggest that future work can use these data and considerations to establish a well-defined simulation of in vitro HBc VLP assembly.

Antigenicity and Immunogenicity Evaluation of HBc VLPs in Mice. Because of the potential to use HBc VLPs as vaccine and drug delivery scaffolds, we next evaluated both the antigenicity and immunogenicity of HBc VLP variants. The HBc protein has been reported to be an important target for antiviral immunity (20). The major antigenic epitopes lie on the outside of the capsid structure, particularly at the tip of spikes. The major immunodominant epitope is the polypeptide T74 to L84 (TNLEDPASRDL; Fig. 5*A*) (21).

The antigenicity of HBc VLPs was examined by enzyme-linked immunosorbent assay (ELISA). Monoclonal antibody C1-5 was used in this assay because it recognizes the T74 to A80 spike epitope. ELISA results (Fig. 5*B*) showed that antibody C1-5 could bind to S-S stabilized HBc VLPs (HBc wild-type SS1 and HBc Original SS1 76AHA) but not the wild-type VLP or the HBc Original 76AHA VLP ("Original" refers to the wild-type P03147 version with nnAA incorporation). Because of low stability, wild-type Original VLPs possibly disassemble in the coating buffer. When coated on the hydrophobic surface of the ELISA plate, the tip of the spike (at the end of a hydrophobic pocket) might therefore become sterically blocked. The SS1 disulfide bridge stabilization avoided disassembly, allowing the stabilized VLP to produce much larger signals in a sandwich-type assay. In contrast, because of the transplant of a new spike into the HBc SS1(HP) 78AHA VLP, it could not be recognized by antibody C1-5. Notably, preexisting HBc-specific antibodies in HBV-infected patients should not interfere with HBc(HP) VLP based vaccines and delivery vehicles. Additionally, VLPs with the nnAA, HPG conjugated to the surface nnAA AHA sites were evaluated to see whether smaller surface modifications would also block C1-5 antibody recognition. The conjugation of HPG abrogated the recognition of HBc antigen protein by antibody C1-5, as shown in Fig. 5*B*.

Ideally, the VLP as a carrier vehicle would induce only a weak or no immune response to avoid suppressing the immunogenicity of conjugated molecules. The immunogenicity of three HPG surface-modified VLPs (HBc Original 76AHA-HPG, HBc Original SS1 76AHA-HPG, and HBc SS1(HP) 78AHA-HPG) was evaluated in mice. It is our general practice to add a small molecular weight alkyne such as HPG during the last stage of our click conjugation reactions. HPG reacts with exposed and unreacted azide groups to avoid the occurrence of nonnatural moieties near the surface of the finished vaccine or drug delivery vehicle. Keyhole limpet hemocyanin (KLH) was used as the positive control because it is the most widely used carrier protein for immunogen preparation (22). All agents were administered three times (at 10-d intervals) with 3-μg doses intradermally. Compared with KLH, the mice injected with VLPs produced low levels of anti-VLP antibodies (<0.6 μg/mL), as shown in Fig. 5*C*. Most notably, the detected anti-VLP antibody levels did not rise

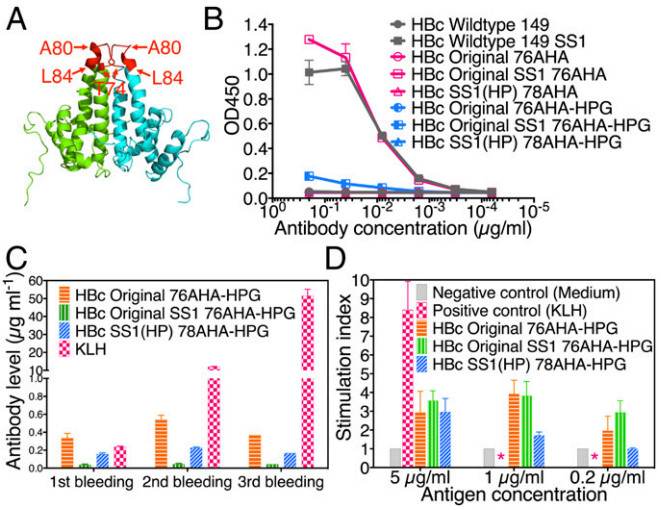

Fig. 5. Antigenicity and immunogenicity of HBc VLPs. (*A*) The main core antigenic loop (red color) at the tip of HBc dimer. (*B*) ELISA of HBc VLPs with antibody C1-5. (*C*) ELISA of mice sera for evaluating the B-cell response. (*D*) Lymphocyte proliferation assay for evaluating the T-cell response. *, data not detected.

even after repeated inoculations, suggesting low humoral immunogenicity. Antigen-specific T-cell responses were evaluated by using a lymphocyte proliferation assay. All three HBc VLPs had a significantly lower stimulation index than KLH (Fig. 5*D*), indicating that the T-cell responses to HBc VLPs were also low. HBc SS1(HP) 78AHA-HPG VLPs had a lower stimulation index than the other two VLPs. The HBc VLP mutant with low intrinsic immunogenicity may allow repeated drug delivery administrations while avoiding neutralizing immune responses and, for vaccines, could avoid diverting vaccine responses away from the desired antigens. Therefore, the stabilized and modified HBc SS1(HP) 78AHA VLP appears to be an excellent vehicle for medical applications.

Conclusion

For the first time, to our knowledge, the HBc VLP was extensively modified to improve its functional properties for important medical applications. Using an *E. coli*-based CFPS system, 10 positions were evaluated for the introduction of artificial disulfide bridges. Introducing cysteines at the D29-R127 position cross-linked both the pentameric and hexameric assembly junctions to augment the intradimer disulfides already present and provided stability even against SDS-mediated disassembly. The new interdimer disulfide bonds will stabilize the VLP during modification, formulation, storage, and administration of vaccines and targeted therapeutics. Moreover, such bonds confer only conditional stability such that the VLPs would be expected to open in the relatively reduced cytoplasmic environment for drug release.

To present molecules on the VLP surface with consistent orientation (much like natural viruses), we introduced non-natural amino acids and used click chemistry. To improve the conjugation efficiencies, we sought to reduce the intense electronegativity on the tip of the protruding surface spikes. However, surprisingly, these mutants assembled poorly. Encouraged that partial charge reduction improved conjugation, we next explored a more radical change: the replacement of the entire surface spike with an extensively modified version from the natural mutant Q8B6N7. This transplantation enabled the assembly of a VLP with essentially no surface charge and with a spike expected to exhibit low antigenicity and immunogenicity. The stabilized and modified new HBc SS1(HP) 78AHA VLP exhibited low immunogenicity in mice and was not recognized by a common anti-HBc antibody. It also enables efficient surface attachment of agents with both positive and negative charge density. This highly engineered VLP demonstrates great promise for medical agents such as vaccines, delivery vehicles, and imaging agents. We suggest that, taken together, this work can now serve as a general paradigm for stabilizing and improving functionality for many VLPs while further exploring the plasticity and structure function relationships of viral capsids.

The developments and findings reported here represent a key step toward understanding and exploring the functional attributes of the HBc capsid. Notably, we uncovered the influence of the HBc spike and its negative charges on capsid assembly and immunogenicity. This observation now suggests new therapeutic opportunities for targeting the HBc spike in HBV infections and may also be relevant for capsids in other viruses.

Materials and Methods

Plasmid Construction. The gene sequence encoding the human HBc antigen (UniProt accession no. P03147) with the C terminus truncated at amino acid 149 was inserted into the pET-24a(+) vector (Novagen). The sequences of HBc constructs are shown in *SI Appendix*.

CFPS. CFPS was conducted by using the PANOx-SP (phosphoenolpyruvate, amino acids, nicotinamide adenine dinucleotide, oxalic acid, spermidine, and putrescine) cell-free system with several modifications (*SI Appendix*). The CFPS products and VLPs were analyzed by SDS/PAGE and autoradiography.

Purification of HBc VLPs. The HBc VLPs were purified by using a Sepharose 6 Fast Flow column (*SI Appendix*). VLPs were analyzed by sucrose gradient sedimentation and transmission electron microscopy. The endotoxins in VLP solutions were removed by phase separation using 0.5% Triton X-114.

Azide-Alkyne Conjugation and Purification. The click reactions were conducted in an anaerobic glovebox. The conjugates were purified by size exclusion chromatography. See *SI Appendix* for details.

Immunization of Mice. Six- to eight-week-old BALB/c mice were obtained and housed at the Laboratory Animal Facility at Stanford University Medical Center. All animal experiments were conducted following the Laboratory Animal Facility and National Institute of Health guidelines. The study protocol was approved by the Stanford University Institutional Animal Care and Use Committee. Ten mice per group were vaccinated intradermally with 3 μg of KLH or HBc VLP formulated in PBS buffer. Blood samples were collected for ELISA, and spleen cells were collected for T-cell proliferation assay (*SI Appendix*).

ACKNOWLEDGMENTS. We thank John P. Welsh, Marcus Rohovie, and Julie A. Fogarty for technical assistance and helpful discussions. We also thank Professor Ronald Levy for assistance with the mouse studies.

1. Hernandez-Garcia A, et al. (2014) Design and self-assembly of simple coat proteins for artificial viruses. *Nat Nanotechnol* 9(9):698–702.
2. Plotkin S (2014) History of vaccination. *Proc Natl Acad Sci USA* 111(34):12283–12287.
3. Cubas R, et al. (2009) Virus-like particle (VLP) lymphatic trafficking and immune response generation after immunization by different routes. *J Immunother* 32(2):118–128.
4. Tissot AC, et al. (2010) Versatile virus-like particle carrier for epitope based vaccines. *PLoS One* 5(3):e9809.
5. Kourtis IC, et al. (2013) Peripherally administered nanoparticles target monocytic myeloid cells, secondary lymphoid organs and tumors in mice. *PLoS One* 8(4):e61646.
6. Clarke BE, et al. (1987) Improved immunogenicity of a peptide epitope after fusion to hepatitis B core protein. *Nature* 330(6146):381–384.
7. Zeltins A (2013) Construction and characterization of virus-like particles: A review. *Mol Biotechnol* 53(1):92–107.
8. Pumpens P, Grens E (2001) HBV core particles as a carrier for B cell/T cell epitopes. *Intervirology* 44(2-3):98–114.
9. Ganem D, Prince AM (2004) Hepatitis B virus infection–natural history and clinical consequences. *N Engl J Med* 350(11):1118–1129.
10. Wynne SA, Crowther RA, Leslie AGW (1999) The crystal structure of the human hepatitis B virus capsid. *Mol Cell* 3(6):771–780.
11. Lu Y, Welsh JP, Chan W, Swartz JR (2013) Escherichia coli-based cell free production of flagellin and ordered flagellin display on virus-like particles. *Biotechnol Bioeng* 110(8):2073–2085.
12. Lu Y, Welsh JP, Swartz JR (2014) Production and stabilization of the trimeric influenza hemagglutinin stem domain for potentially broadly protective influenza vaccines. *Proc Natl Acad Sci USA* 111(1):125–130.
13. Zawada JF, et al. (2011) Microscale to manufacturing scale-up of cell-free cytokine production–a new approach for shortening protein production development timelines. *Biotechnol Bioeng* 108(7):1570–1578.
14. Patel KG, Swartz JR (2011) Surface functionalization of virus-like particles by direct conjugation using azide-alkyne click chemistry. *Bioconjug Chem* 22(3): 376–387.
15. Kanter G, et al. (2007) Cell-free production of scFv fusion proteins: An efficient approach for personalized lymphoma vaccines. *Blood* 109(8):3393–3399.
16. Ohto U, et al. (2015) Structural basis of CpG and inhibitory DNA recognition by Toll-like receptor 9. *Nature* 520(7549):702–705.
17. Alexander CG, et al. (2013) Thermodynamic origins of protein folding, allostery, and capsid formation in the human hepatitis B virus core protein. *Proc Natl Acad Sci USA* 110(30):E2782–E2791.
18. UniProt Consortium (2014) Activities at the Universal Protein Resource (UniProt). *Nucleic Acids Res* 42(Database issue, D1):D191–D198.
19. Punta M, et al. (2012) The Pfam protein families database. *Nucleic Acids Res* 40(Database issue):D290–D301.
20. Chen MT, et al. (2004) A function of the hepatitis B virus precore protein is to regulate the immune response to the core antigen. *Proc Natl Acad Sci USA* 101(41): 14913–14918.
21. Homs M, et al. (2011) HBV core region variability: Effect of antiviral treatments on main epitopic regions. *Antivir Ther* 16(1):37–49.
22. Harris JR, Markl J (1999) Keyhole limpet hemocyanin (KLH): A biomedical review. *Micron* 30(6):597–623.